CORROSION BEHAVIOR OF EXPERIMENTAL AND COMMERCIAL NICKEL-BASE ALLOYS IN HCl AND HCl CONTAINING Fe^{3+}

Gordon R. Holcomb, Bernard S. Covino Jr., Sophie J. Bullard, Malgorzata Ziomek-Moroz, Thomas A. Adler, Steven A. Matthes, David E. Alman, and Paul D. Jablonski
Albany Research Center, U.S. Department of Energy
1450 Queen Avenue SW, Albany, OR 97321
holcomb@alrc.doe.gov

ABSTRACT

The effects of ferric ions on the corrosion resistance and electrochemical behavior of a series of Ni-based alloys in 20% HCl at 30ºC were investigated. The alloys studied were those prepared by the Albany Research Center (ARC), alloys J5, J12, J13, and those sold commercially, alloys 22, 242, 276, and 2000. Tests included mass loss, potentiodynamic polarization, and linear polarization.

INTRODUCTION

Hydrochloric acid (HCl) is second to sulfuric acid in the numerous and diverse applications of the manufacturing and synthetic chemical industry. It is an extremely corrosive and aggressive acid depending on its concentration, temperature, and oxidizing impurities. A couple of uses are the pickling and chemical cleaning of steel in pharmaceutical industries.[1]

In such applications in the chemical process industry, steel (including stainless steel), and copper alloys cannot generally tolerate exposure to HCl; therefore, the use of nickel alloys is essential. These alloys possess the ability to passivate in the presence of HCl,[1-2] yet in many cases high HCl concentrations or high temperatures can disrupt the alloy's passive state.[1]

The Ni-Cr-Mo alloy group has been shown to be one of the most versatile alloy groups and particularly corrosion resistant in aqueous solutions.[1-2] The commercial alloys studied include Haynes-242(1), Hastelloy-C22(1), -C276(1), and -C2000(1) and are henceforth referred to as 242, 22, 276, and 2000. The Albany Research Center (ARC) of the U.S. Department of Energy has developed a set of Ni-base alloys, J5, J12, and J13, whose alloying content is similar in many respects to the commercial alloys. The compositions of the alloys are shown in Table 1.

(1) Trademark

TABLE 1
NOMINAL ALLOY COMPOSITION OF TEST ALLOYS (WT%, BALANCE Ni)

Alloy Name	UNS	Cr	Mo	Mn	Ti	Al	Fe	Co	Cu	Si	Other
242	N10242	7.0-9.0	24.0-26.0	<0.80		<0.50	<2.0	<2.5	<0.50	<0.80	<0.03 C <0.006 B
22	N06022	22	13	<0.50			3	<2.5		<0.08	3 W <0.010 C <0.35 V
276	N10276	16	16	<1			5	<2.5		<0.08	4 W <0.35 V <0.01 C
2000	N06200	23	16						1.6	<0.08	<0.01 C
J5		12.5	22.0	0.5	1	0.1					0.1 Y
J12		10.0	20.0	0.5	1	0.1					0.1 Y
J13		8.0	18.5	0.5	1	0.1					0.1 Y

The work presented here is a comparison between commercially available nickel alloys and newly developed ARC alloys. The purpose was to investigate the electrochemical behavior and corrosion resistance of the alloys in solutions of 20 % HCl and 20% HCl plus 700 ppm ferric ions (Fe^{3+}) at 30°C. It was of interest to better understand the general corrosion properties of the ARC alloys for possible future applications.

EXPERIMENTAL PROCEDURE

Materials

The commercial alloys selected for this research, 242, 22, 276, and 2000, are extensively used in the chemical processing industry as well as pollution control and waste treatment industries. Having both chromium and molybdenum as alloying metals gives these alloys the ability to be used in both oxidizing and non-oxidizing applications. The ARC developed alloys, J5, J12, and J13, were not initially developed for the use in corrosive aqueous environments, but rather for high temperature gaseous environments. The fabrication and modification of these alloys was designed to increase formability and efficiency as well as to reduce the cost of low coefficient of thermal expansion nickel-base superalloys. Their primary use is intended for interconnect applications in intermediate temperature solid oxide fuel cells.[3] These alloys were used in the current research to further understand their behavior and to extend their applications.

Sample Preparation

Each sample coupon was machined to approximately 1 x 0.5 in (2.5 x 1.25 cm) with a 0.125 in (0.32 cm) diameter hole near the one of the short edges. Coupon thickness was approximately 0.04 cm for J5, J12 and J13, and approximately 0.15 cm for 242, 22, 276 and 2000. All sample surfaces and edges were polished to a 600-grit finish and engraved with the alloy type and designated sample number. Before the mass loss test, samples were cleaned with methanol in an ultrasonic cleaner and then air-dried. Density measurements of each alloy were taken using an ultrapycnometer. Every sample was initially weighed and the surface area calculated.

Mass Loss Test

The alloy samples were tested by immersion in solutions of 20% HCl and 20% HCl plus 700 ppm ferric ions added in the form of ferric chloride salt ($FeCl_3 \bullet 6H_2O$). Each solution was deaerated with nitrogen both prior to testing and during testing. The alloys were exposed to the solutions for 1, 7, and 14 days at a temperature of 30 $\pm$ 1°C. After each exposure interval the samples were weighed to determine the mass loss. The mass loss, surface area, exposure time, and alloy density were then used to calculate a corrosion penetration rate in units of mils per year (mpy) and millimeters per year (mm/y).

Electrochemical Test

Electrochemical tests were performed in a standard three-electrode flat cell. Tests performed included linear polarization resistance (LPR) and potentiodanymic polarization techniques. The reference electrode used to measure the electrochemical potential was a saturated calomel electrode (SCE). The solutions used were 20% HCl and 20% HCl containing 700 ppm ferric ions in the form of ferric chloride salt ($FeCl_3 \bullet 6H_2O$). Each solution was purged with nitrogen gas for approximately thirty minutes to deaerate the solution before performing the test and then throughout the remainder of the test. A open-circuit-potential (OCP) test was performed before each of the LPR and potentiodynamic tests. The LPR measurements were conducted over an interval of ±15 mV, while the potentiodynamic polarization was started at –300 mV vs OCP to 1400 mV vs SCE. Both tests were run at a scan rate of 100 mV/min.

Specimen Morphology

Selected corroded mass loss samples were examined using a JEOL-7000F field emission scanning electron microscope (SEM). Samples examined were J5, J12, and J13 exposed to 20% HCl plus 700 ppm Fe^{3+} ions for 14 days.

RESULTS AND DISCUSSION

Mass Loss Tests

<u>20% HCl Solution:</u> As can be seen in Fig. 1 and Table 2, ARC alloys J12 and J13 and the commercial alloy 242 exhibited a decrease in corrosion rate to less than 0.2 mpy as the exposure time approached 14 days. These alloys all had Cr concentrations of 10 wt% or less, and Mo concentrations above 18 wt%.

Molybdenum is reported to help protect alloys against this environment and enhances the corrosion resistance.[1,4] The cathodic reaction taking place in 20% HCl is

$$2H^+ + 2e^- \rightarrow H_2 \quad (1)$$

Protons (H^+) accept electrons generated by the anodic reaction (Eq. 2), thus enhancing the dissolution of the metal:

$$Ni \rightarrow Ni^{2+} + 2e^- \quad (2)$$

20% HCl with 700 ppm Fe^{3+}:

Ferric ions were added to 20% HCl to investigate its effect on the corrosion behavior of the nickel base alloys. The presence of ferric ions in solution creates a more oxidizing environment. In this solution there are two reduction reactions taking place on the surface of the metal, reduction of hydrogen, Eq. 1, and ferric ions to ferrous ions, Eq. 3.

$$Fe^{3+} + e^{-} \rightarrow Fe^{2+} \quad (3)$$

In some cases, ferric ions can inhibit the formation of a passive film resulting in active dissolution of the material and transpassive behavior,[5] which can lead to the formation of ions with higher oxidation states such as Ni^{3+}, Mo^{6+}, and Cr^{6+}. After the alloy coupons were exposed to the solution a noticeable change occurred on the surface. The coupons showed a rough surface with a gray dull appearance. This may indicate that an etching process took place.

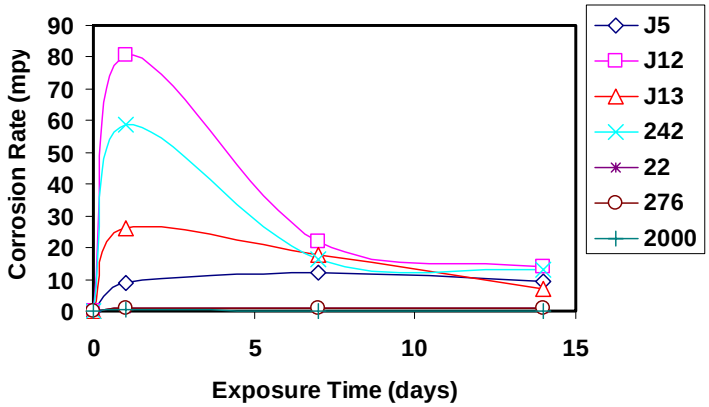

FIGURE 1 – Mass loss behavior in 20% HCl at 30°C.

TABLE 2
CORROSION RATES (mpy) IN 20% HCl AT 30°C

Alloy	1 day	7 days	14 days
242	0.14	0.10	0.07
22	1.12	1.11	0.77
276	0.54	0.41	0.77
2000	0.28	0.36	0.45
J5	0.04	0.32	0.42
J12	0.24	0.15	0.11
J13	0.24	0.10	0.11

In these oxidative conditions, alloys with high concentrations of chromium were the most protective, as shown in Fig. 2. Figure 2 and Table 3 show that 22 and 2000 had the lowest corrosion rate of about 0.06 mpy after 14 days. Alloy 276 had good corrosion protection with a rate of 0.85 mpy after 14 days, while 242, J5, J12, and J13 all had higher corrosion rates of more than 6 mpy after 14 days.

The demonstrated corrosion resistance of higher chromium alloys is the result of the formation of a chromium oxide passive film on the surface of the alloy.[1] Alloys higher in molybdenum like J5 are not as corrosion resistant, possibly due to second phase precipitates rich in Mo in the matrix. Deposition of Mo along the alloy surface enhances corrosion rates by blocking dissolution sites when exposed to a corrosive environment.[1]

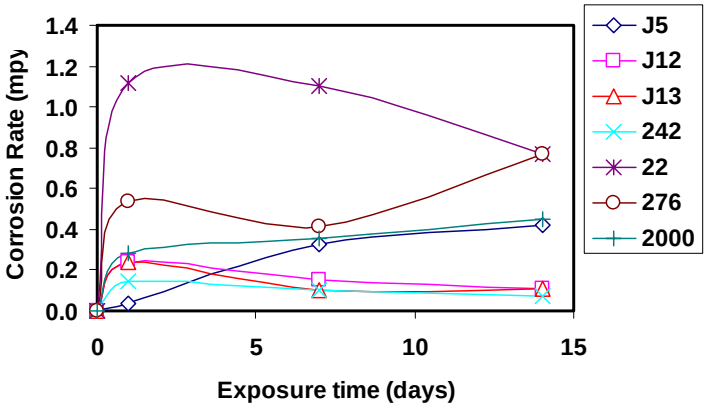

FIGURE 2 – Mass Loss behavior in 20% HCl with 700 ppm Fe^{3+} at 30°C.

TABLE 3
CORROSION RATES (mpy) IN 20% HCl WITH 700 PPM Fe^{3+} AT 30°C

Alloy	1 day	7 days	14 days
242	58.79	16.21	13.06
22	0.32	0.02	0.06
276	0.91	0.83	0.85
2000	0.29	0.02	0.06
J5	8.87	12.12	9.25
J12	135.99	22.11	14.18
J13	26.00	17.57	6.90

Taking into account the electrochemical nature of corrosion of Ni-based alloys in HCl and HCl containing Fe^{3+}, corrosion rates, in terms of corrosion current density, can be predicted using the mixed potential theory along with the Tafel equations. When a Ni-based alloy is corroding in HCl, anodic and cathodic half-cell reactions occur simultaneously on the surface. Each half-cell reaction has its own half-cell electrode potential and exchange current density. During the corrosion process, the two half-cell electrode potentials $E_{Ni2+/Ni}$ and $E_{H2+/H2}$ cannot coexist separately on an electrically conductive surface. Therefore, each changes potential, due to polarization, to reach the same potential value, which is the corrosion potential, E_{corr}. At E_{corr} the rates of the cathodic (Eq. 1) and anodic (Eq. 2) reactions are equal, e.g., $i_c=i_a=i_{corr}$. Figure 3a shows a polarization diagram for corrosion of metal M, controlled by activation polarization, in a acidic solution that provides H^+ for the cathodic half-cell reaction.[5]

Higher corrosion rates of the investigated materials observed in HCl containing Fe^{3+} than those in HCl, can also be explained using the mixed potential theory together with the Tafel equations. In the absence of Fe^{3+}, the corrosion rate of Ni is given by the intersection of hydrogen-reduction and metal dissolution polarization curves. The addition of Fe^{3+}, which is a strong oxidizer, shifts the corrosion potential to E_{corr} and consequently increases corrosion rate from i'_{corr} to i_{corr} and decreases hydrogen evolution from i'_{corr} to $i_{H+\rightarrow H2}$ as shown schematically in Figure 3b.[5]

Electrochemical Measurements

The results of electrochemical measurements, namely potentiodynamic polarization, are shown in Fig. 4, with the commercial alloys in Figs. 4a-4d and the ARC alloys in Figs. 4e-4g. The electrochemical values, such as corrosion potential (E_{corr}), corrosion current density (i_{corr}), Tafel constants (βa & βc), and corrosion rate are listed in Table 4 for the 20% HCl solution and in Table 5 for the 20% HCl with 700 ppm Fe^{3+} solution. The corrosion rates taken from the potentiodynamic and the linear polarization (R_p) tests are shown in Table 6 as "Tafel Fit" and "R_p Fit", respectively.

The compositions of the ARC series of alloys (J5, J12, and J13) are very similar to each other, where the only change in alloying is between nickel, chromium and molybdenum content. As previously mentioned, the Ni-Cr-Mo alloys have the ability to be used in both oxidizing and non-oxidizing solutions. As the chromium content increases the corrosion resistance in an oxidizing solution increases, while an increase in molybdenum will increase the corrosion resistance in a reducing solution. As shown in Tables 4 and 5, these alloying properties did affect the corrosion resistance in each solution.

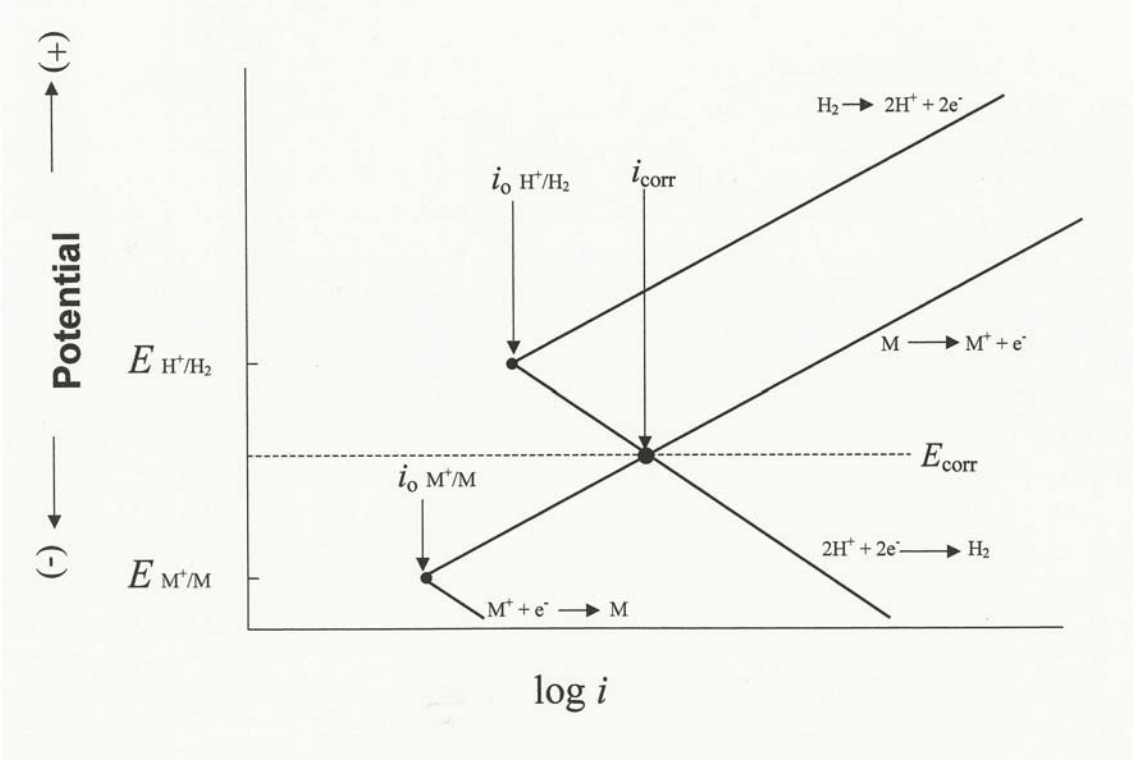

a)

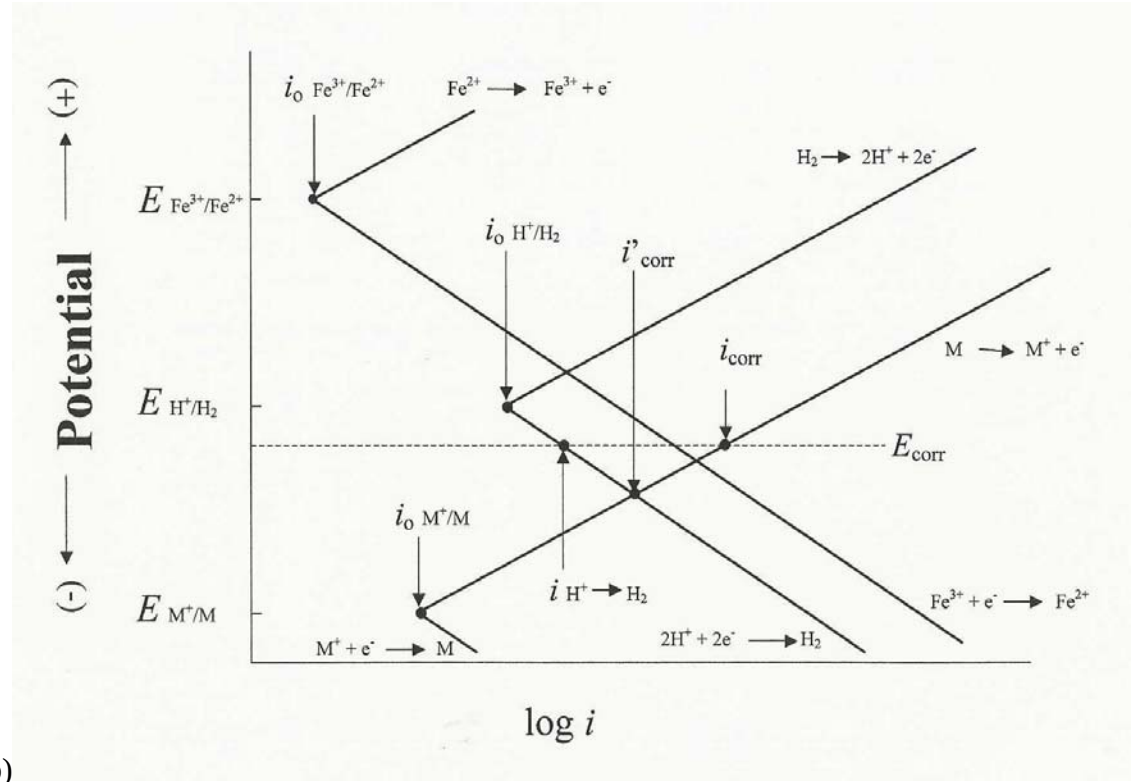

b)

FIGURE 3 – a) Polarization diagram for corrosion of metal M, controlled by activation polarization, in an acidic solution that provides H^+ for the cathodic half-cell reaction.[5] b) The addition of Fe^{3+}, which is a strong oxidizer, shifts the corrosion potential to E_{corr} and consequently increases the corrosion rate from i'_{corr} to i_{corr} and decreases hydrogen evolution from i'_{corr} to $i_{H+\rightarrow H2}$.[5]

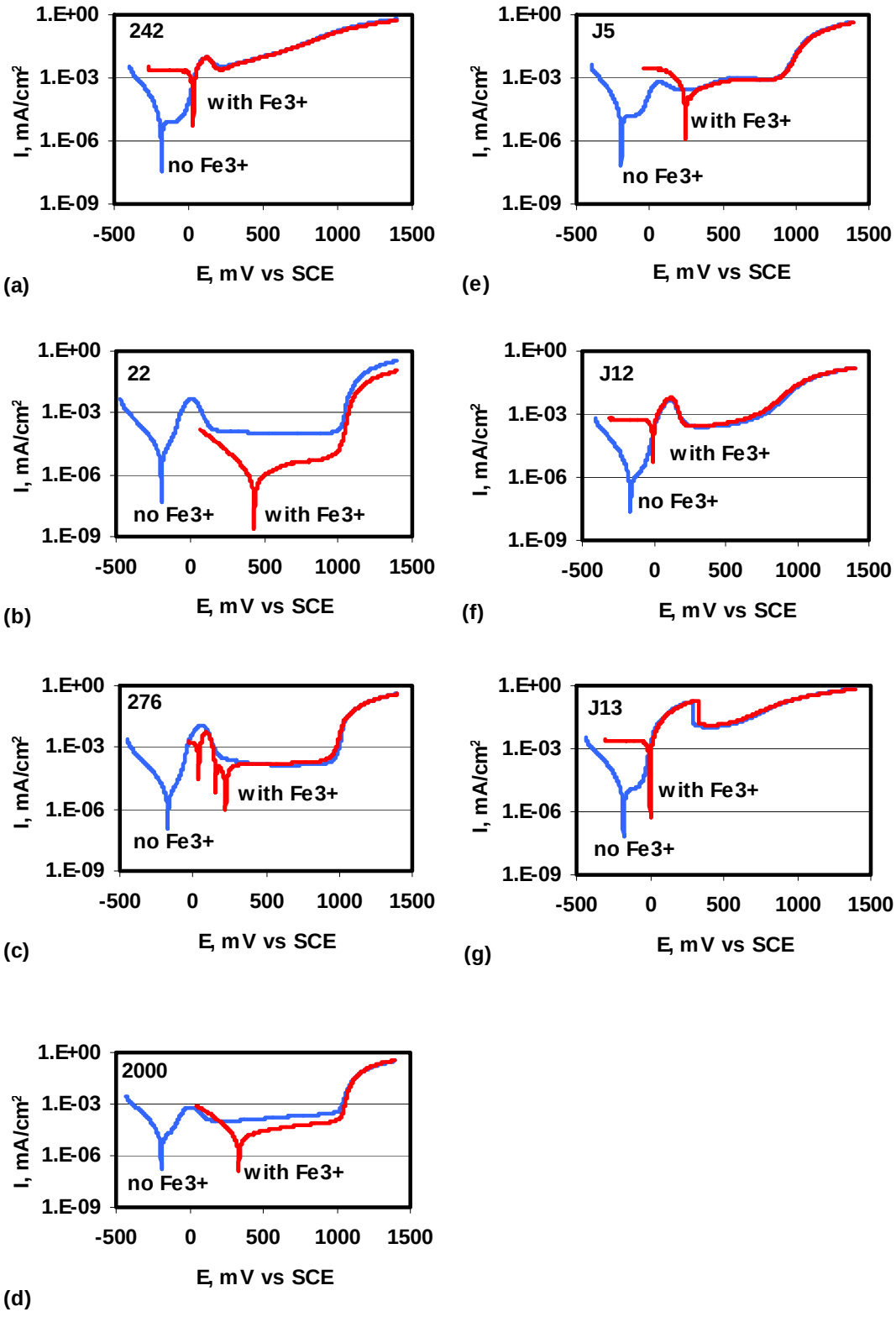

FIGURE 4 – Potentiodynamic polarization results in 20% HCl solutions both with and without 700 ppm Fe^{3+}. Temperature was 30°C.

TABLE 4
ELECTROCHEMICAL VALUES IN 20% HCl

Alloy	βa (mV)	βc (mV)	i_{corr} (A/cm²)	E_{corr} (mV)	Corrosion Rate mpy	mm/y
242	110.39	36.37	3.78E-06	-181	1.88	0.05
22	71.23	61.31	5.48E-06	-195	2.73	0.07
276	85.44	66.85	3.54E-06	-172	1.62	0.04
2000	131.68	86.96	1.15E-05	-192	5.48	0.14
J5	120.82	41.67	7.37E-06	-194	3.61	0.09
J12	120.83	48.05	1.89E-06	-162	0.93	0.02
J13	109.67	50.13	3.79E-06	-178	1.86	0.05

TABLE 5
ELECTROCHEMICAL VALUES IN 20% HCl with 700 ppm Fe^{3+}

Alloy	βa (mV)	βc (mV)	i_{corr} (A/cm²)	E_{corr} (mV)	Corrosion Rate mpy	mm/y
242	53.05	113.38	8.13E-04	32	405.44	10.30
22	105.61	86.04	8.61E-07	440	0.44	0.01
276	48.37	105.90	7.82E-04	38	357.63	9.08
2000	151.70	94.62	5.61E-06	337	2.68	0.07
J5	160.60	91.80	9.25E-05	246	45.29	1.15
J12	52.38	103.70	6.90E-04	-6	339.18	8.62
J13	47.53	99.50	7.93E-04	-1	388.23	9.86

TABLE 6
CORROSION RATE VALUES (mpy) FROM POTENTIODYNAMIC ANALYSIS AND LINEAR POLARIZATION

	20% HCl		20% HCl with 700 ppm Fe^{3+}	
Alloy	Tafel Fit	R_p Fit	Tafel Fit	R_p Fit
242	1.88	1.09	405.44	816.45
22	2.73	2.64	0.44	5.44
276	1.62	3.05	357.63	21.85
2000	5.48	3.40	2.68	1.52
J5	3.61	2.88	45.29	67.97
J12	0.93	2.90	339.18	891.58
J13	1.86	2.35	388.23	1200.40

20% HCl Solution: In this solution all anodic and cathodic reactions were activation controlled. That is, there was no evidence of diffusion control, as temperature (activation) had the primary influence in the reaction rate, while all other factors stayed the same. All alloys

showed different features of passivity with J13, 242, and perhaps J5 being pseudo-passive as illustrated in Figure 4. This can be attributed to the levels of current in the passive region. The formation of this pseudo-passive film can be attributed to the formation of molybdenum dioxide and/or molybdenum trioxide under these conditions.[1] J13 appeared to be the least passive of the alloys.

20% HCl + 700 ppm Fe^{3+} Solution: Figure 4 shows that all alloys were drastically affected by the presence of an oxidizer (Fe^{3+}). In this solution the cathodic reactions are predominantly diffusion controlled with the exception of 22 and 2000, which are two of the alloys with the highest amount of chromium. All alloys showed the beginning of transpassive corrosion at about 1000 mV SCE. This value sets the upper limit of potential at which the alloys are usable. As demonstrated in Figure 4, all curves showed that upon the addition of ferric ions, an oxidizer can shift the corrosion potential to more positive potentials. Alloys J5, 2000, and 22 showed the most noticeable shifts with a change of Ecorr of approximately 440mV, 529mV, and 635mV, respectively.

Comparison of ARC alloys with Commercial Alloys: Alloy J5 was most similar to 22 and 2000 as illustrated in Figures 5 and 6. Alloy J5 had the highest chromium content within the ARC alloys. Alloys J12 and J13 were most similar to 242, as illustrated in Figs. 5-6. Alloys J12 and 242 had almost identical E_{corr} and i_{corr} values, and very similar behavior in both solutions.

Scanning Electron Microscopy (SEM) Analysis

The surface morphologies of J5, J12, and J13 due to 14-day exposure in the oxidizing solution are illustrated in Figure 7. These micrographs were taken using backscatter electrons at a magnification of 500X (a and b) and 1000X (c). Molybdenum second phase precipitates (confirmed with energy dispersive spectroscopy) were clearly present in J5 and J13, while in J12 they were rarely seen other than at much higher magnifications. These second phase precipitates are most clearly seen as the white rounded particles in Figure 7c. Each alloy demonstrated a corrosion microstructure consistent with an etch process.

A number of Ni-Cr-Mo alloys form mu, P, sigma, and carbide phases.[6-10] These phases are rich in Mo and/or Cr, and when they form, the matrix is depleted in Mo and/or Cr. The two phases, mu and P, are rich in Mo, while sigma is rich in Cr and Mo.[9-10] Since Cr and Mo are added to the Ni alloys to impart corrosion resistance, the depleted matrix can be prone to localized corrosion.[7-8] However, no localized corrosion was observed.

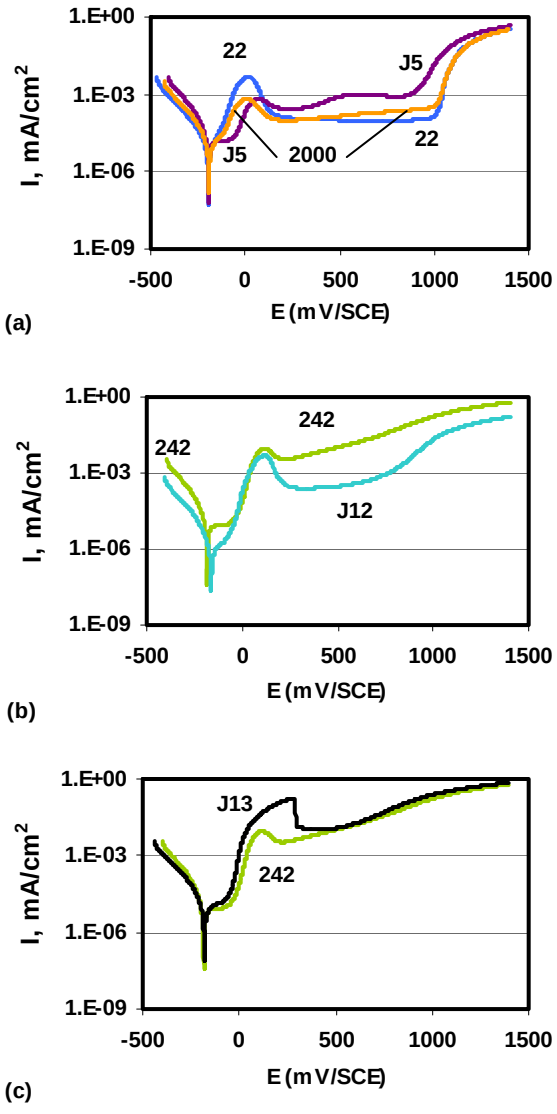

FIGURE 5 – Potentiodynamic polarization results in 20% HCl solutions comparing commercial and ARC alloys. Temperature was 30°C.

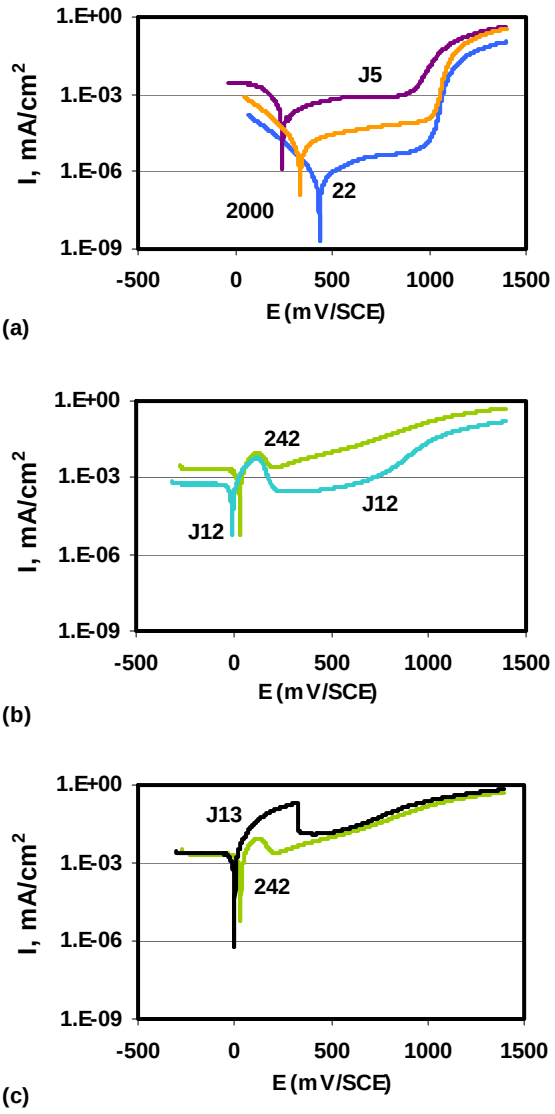

FIGURE 6 – Potentiodynamic polarization results in 20% HCl with 700 ppm Fe^{3+} solutions comparing commercial and ARC alloys. Temperature was 30°C.

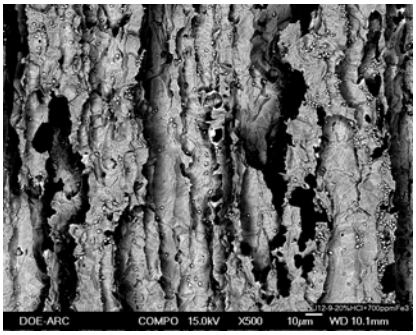

a)

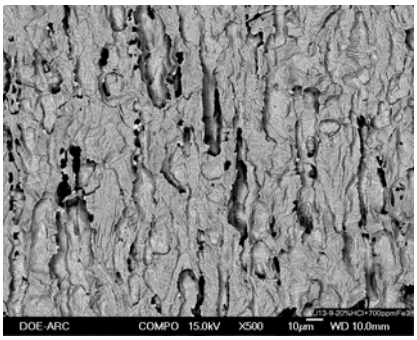

b)

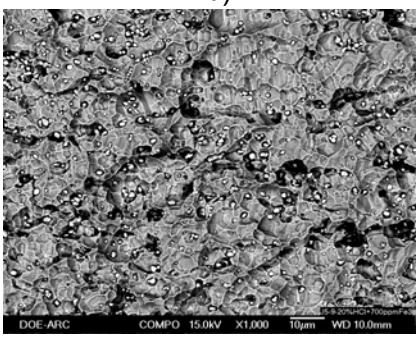

c)

FIGURE 7 - Backscatter electron micrographs showing the corroded surface of a) J5 (original at 500X), b) J12 (original at 500X), and c) J13 (original at 1000X) after exposure to 20% HCl with 700 ppm Fe3+ for 14 days at 30°C. All markers are 10μm.

CONCLUSIONS

- Alloys with both high concentrations of Mo and low concentrations of Cr, such as 242, J13, and J12, exhibited low corrosion rates in 20% HCl at 30°C.

- Increasing the oxidation potential of the solution by the addition of ferric ions to 20% HCl caused a dramatic change in the corrosion behavior of all ARC alloys. These alloys exhibited similar corrosion rates under this strong oxidizing environment. J5 possessed the higher resistance to corrosion within the ARC alloys, although all the high Cr commercial alloys performed better.

- Alloys with higher chromium content showed the best corrosion rates in the oxidizing solution.

- J5 showed electrochemical behavior similar to 22 and 2000 although the commercial alloys had lower corrosion rates in the oxidizing solution.

- J12, J13, and 242 had similar electrochemical behavior in both solutions.

- All commercially available alloys, with the exception of 242, demonstrated better corrosion resistance in the oxidizing solution than the ARC alloys.

ACKNOWLEDGEMENTS

The authors wish to thank the efforts of Isaac A. Anchondo and Marissa E. Morales during this project. They were both a part of the Mickey Leland Energy Fellowship summer intern program at the Albany Research Center in 2005.

REFERENCES

1. N. S. Meck, P. Crook, D. L. Klarstrom, R. B. Rebak, “Effect of Ferric ions on the Corrosion Performance of Nickel Alloys in Hydrochloric Acid Solutions,” CORROSION/04, paper no. 04430 (Houston, TX: NACE International, 2004).
2. N. S. Meck, P. Crook, D. L. Klarstrom, R. B. Rebak, “Electrochemical Behavior of Nickel Alloys in HCl Solutions containing Oxidizing Impurities,” CORROSION/05, paper no. 05334 (Houston, TX: NACE International, 2005).
3. D. E. Alman, P. D Jablonski, “Low Coefficient of Thermal Expansion (CTE) Nickel Base Superalloys for Interconnect Applications in Intermediate Temperature Solid Oxide Fuel Cells (SOFC),” in Superalloys-2004 (Warrendale, PA: TMS, 2004), pp. 617-622.
4. R. B. Rebak, “Effects of Metallurgical Variables on the Corrosion of High-Nickel Alloys,” in Corrosion: Fundamentals, Testing, and Protection, ASM Handbook Vol. 13A (Materials Park, OH: ASM International, 2003), pp. 279-286.
5. M. G. Fontana, Corrosion Engineering, 2nd Ed, (New York, NY: McGraw-Hill, 1978), pp. 316-326.
6. S. Dymek, M. Dollarand M, Farooqi, “Optimization of Mechanical Properties of a Ni-Mo-Cr alloy by Structural modifications induced by changes in heat treatment,” Materials Science and Engineering, A319-321 (2001): pp. 284-289.
7 J. R. Crum, J. M. Pole, E. L. Hibner, “Corrosion Resistant Nickel-Chromium-Molybdenum Alloys,” U.S. Patent Number 5,019,184 (1991).
8. P. Crook, “Copper-Containing Ni-Cr-Mo Alloys,” U.S. Patent Number 6,280,540 (2001).
9. M. Raghavan, R. R. Mueller, G. A. Vaughn, S. Floreen, “Determination of Isothermal Sections of Nickel Rich Portion of Ni-Cr-Mo System by Analytical Electron Microscopy,” Metallurgical Transactions, 15A (1984): pp. 783-792.
10. E. Gozlan, M. Bamberger, S. F. Dirnfeld, B. Prinz and J. Klodt, “Topologically close-packed precipitates and Phase diagrams of Ni-Cr-Mo and Ni-Mo-Fe and Ni-Mo-Fe with constant additions of chromium,” Materials Science and Engineering, A141 (1991): pp. 85-95.